The crystal structure and low-magnetic-field properties of the Pb- and Ba-doped Bi-Sr-Ca-Cu-O system

1991 J. Phys.: Condens. Matter 3 9481

(http://iopscience.iop.org/0953-8984/3/47/020)

J. Phys.: Condens. Matter 3 (1991) 9481–9488. Printed in the UK

The crystal structure and low-magnetic-field properties of the Pb- and Ba-doped Bi–Sr–Ca–Cu–O system

Mao Zhiqiang†, Zeng Xinglin‡, Yang Li†, Wang Yu‡, Wang Shunxi‡, Cao Leizhao‡, Chen Zhaojia‡, Fan Chenggao† and Zhang Yuheng†§

† Center of Structure and Element Analysis, University of Science and Technology of China, 230026 Hefei, Anhui, People's Republic of China

‡ Department of Physics, University of Science and Technology of China, 230026 Hefei, Anhui, People's Republic of China

§ CCAST (World Laboratory), PO Box 8730, Beijing, People's Republic of China

Received 3 April 1991, in final form 1 July 1991

Abstract. The XRD analyses for the Bi–Pb–Sr–Ca–Ba–Cu–O system show that the addition of Ba ions is favourable to the formation of the higher-T_c phase ($T_c > 100$ K), and TEM observations show that the partial substitution of Ba ions for Ca ions induces a change in the crystal microstructure of the higher-T_c phase ($T_c > 100$ K); a new modulation mode with a wavelength of 43 Å appears in the electron diffraction pattern of the higher-T_c phase. The EDS results confirm that Ba ions really intercalate into the crystal of the 2:2:2:3 phase. The DC magnetization measurements show that the sample displays a much larger hysteresis than that of a general Pb-doped sample. In addition, a study on the influence of low DC magnetic fields on the real component χ' and imaginary component χ'' of the susceptibility for the Ba-doped sample shows that T_p is related to the applied field H^{DC} and their relation can be fitted by $(1 - T_p/T_c) \propto H^{0.23}$ when $H^{DC} < 140$ G, and $(1 - T_p/T_c) \propto H^{0.65}$ when $H^{DC} > 140$ G. These data can be excellently interpreted in terms of Bean's critical-state model.

1. Introduction

After Maeda *et al* [1] discovered two superconducting phases in the Bi–Sr–Ca–Cu–O system, it was reported by some groups [2–4] that the lower-T_c phase ($T_c \cong 80$ K) was identified as $Bi_2Sr_2CaCu_2O_8$, while the higher-T_c phase ($T_c > 100$ K) was considered to have the ideal composition $Bi_2Sr_2Ca_2Cu_3O_{10}$. In order to obtain single-phase samples with $T_c > 100$ K, extensive investigations have been carried out. It has been revealed that the partial substitution of Pb for Bi is effective in increasing the volume fraction of the higher-T_c phase [5], and the substitution of antimony in the Bi–Pb–Sr–Ca–Cu–O system can also accelerate the formation of the higher-T_c phase [6]. Yanagisawa *et al* [7] reported that the volume fraction of the higher-T_c phase could be increased by prolonged sintering. Recently, we added Ba, one of the alkaline-earth metals, to the Bi–Pb–Sr–Ca–Cu–O system, and also obtained a nearly pure higher-T_c phase ($T_c > 100$ K) sample, i.e. the addition of Ba ions can also facilitate the formation of the higher-T_c phase. Subsequently, we studied in particular the low-magnetic-field properties of the Ba-doped sample by measurements of the complex AC susceptibility and DC magnetization and simultaneously investigated its crystal structure by means of TEM observations and

0953-8984/91/479481 + 08 $03.50

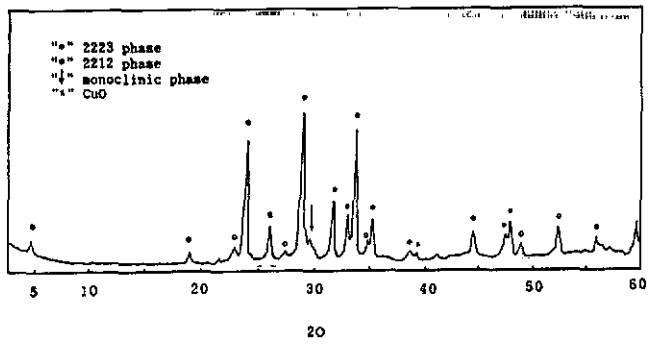

Figure 1. X-ray diffraction pattern for the $Bi_{1.7}Pb_{0.3}Sr_2Ca_{1.8}Ba_{0.2}Cu_3O_y$ sample.

XRD analyses. In this paper, we present our experimental results obtained for this sample and discuss, with emphasis, the influence of low DC magnetic fields ($H^{DC} \leq 300$ G) on the real component χ' and imaginary component χ'' of the susceptibility.

2. Sample preparation and experimental methods

A sample with the nominal composition $Bi_{1.7}Pb_{0.3}Sr_2Ca_{1.8}Ba_{0.2}Cu_3O_y$ was prepared by solid state reaction in air. Thestarting materials were high-purity powders of Bi_2O_3, PbO, $SrCO_3$, $BaCO_3$ and CuO. Appropriate amounts of these powders were mixed, ground and pre-heated at 820 °C for 20 h. Next they were ground again and pressed into a pellet 10 mm in diameter; then the pellet was sintered at 850 °C for 80 h and finally quenched in air.

An x-ray powder diffraction experiment was performed on a Ligaku D/MAX-γA diffractometer using monochromatic high-intensity Cu Kα radiation at room temperature. The AC susceptibility was measured with a mutual inductance bridge as a function of temperature. The frequency f of the applied AC field was 119 Hz, and the exciting field amplitude H_m was 0.05 Oe. A low DC magnetic field ($H^{DC} \leq 300$ G) was applied parallel to the AC magnetic field. The DC magnetization was measured with a ballistic galvanometer connected to opposite-series pick-up coils. The magnetic field which was produced by a copper solenoid cooled by liquid nitrogen was parallel to the axis of sample. The temperature dependence of resistivity was obtained using the standard four-probe technique. A study of the crystal microstructure and analyses of the energy-dispersive spectrum on this sample was made with an H-800 transmission electron microscope.

3. Results and discussion

Figure 1 shows the x-ray diffraction pattern of the sample with the nominal composition $Bi_{1.7}Pb_{0.3}Sr_2Ca_{1.8}Ba_{0.2}Cu_3O_y$ (denoted as sample A below). It is very obvious that the intensities of the characteristic diffraction peak series of the higher-T_c phase ($T_c > 100$ K) (as shown by full circles in figure 1) are much larger than those of the lower-T_c phase ($T_c \cong 80$ K) (as shown by open circles in figure 1) and other impurity phases which

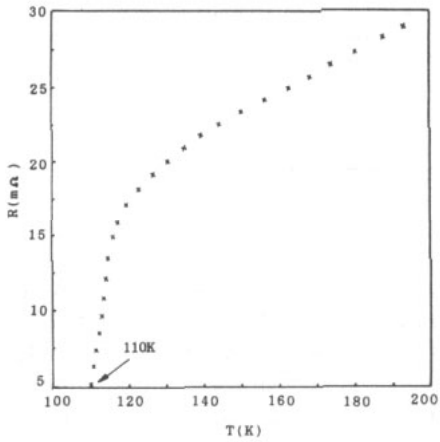

Figure 2. Resistance versus temperature for the $Bi_{1.7}Pb_{0.3}Sr_2Ca_{1.8}Ba_{0.2}Cu_3O_y$ sample.

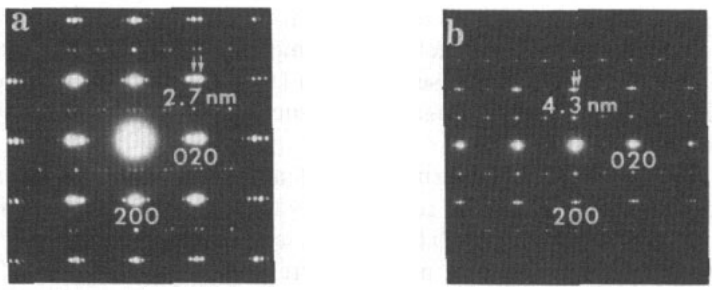

Figure 3. (*a*) Electron diffraction pattern for the $Bi_{1.7}Pb_{0.3}Sr_2Ca_2Cu_3O_y$ sample. (*b*) Electron diffraction pattern for the $Bi_{1.7}Pb_{0.3}Sr_2Ca_{1.8}Ba_{0.2}Cu_3O_y$ sample.

contain the monoclinic phase (indicated by an arrow) identified in our early work [8] and CuO (indicated by a cross), i.e. the 110 K phase in the sample is apparently dominant. Moreover this sample also displays better superconductivity with a zero-resistance temperature of 110 K, as shown in figure 2. All this suggests that the presence of Ba enhances the formation of the higher-T_c phase.

Figure 3(*b*) shows the typical electron diffraction pattern of sample A. With a view of the comparison with sample A, the electron diffraction pattern of the sample $Bi_{1.7}Pb_{0.3}Sr_2Ca_2Cu_3O_y$ (sample B), which does not contain Ba, is also exhibited in figure 3(*a*). The preparation conditions for the two samples are the same. The two pictures indicate that the strong spots due to the fundamental reflection are identical for the two samples; however, the patterns of the weak spots due to superstructure reflection are quite different. It should be noted that a new kind of incommensurate modulation mode along the *b* axis appears for sample A, as shown in figure 3(*b*), and its wavelength is calculated to be 4.3 nm, while only the conventional modulation [9] is observed for sample B, as shown in figure 3(*a*).

The chemical compositions of sample A measured by EDS are shown in table 1. From this table, it can be seen that the sample is Bi and Pb rich and Sr poor compared with the ideal composition of the 110 K phase (2:2:2:3), furthermore, a small number of Ba ions is really intercalated into the crystal of the 2:2:2:3 phase. It is known that the

Table 1. Cationic compositions of Bi–Pb–Sr–Ca–Ba–Cu–O as measured by EDS.

Element	Bi	Pb	Sr	Ca	Ba	Cu
Amount, mean value (at.%)	26.6	6.5	15.3	20.5	1.1	30.0
Amount, range (at.%)	25.9–28.6	6–6.9	14.9–16.4	18.9–21.8	0.7–1.3	29.2–30.5

double Bi_2O_2 layers do not consist of perfect two-dimensional sheets but contain an alternate distribution of Bi-concentrated bands and Bi-deficient bands, and local contraction and dilation of atomic chains appear relevantly between BiO layers [10, 11]. According to the above composition analyses, which suggest that some vacancies must exist in Sr sites, it can be thought that the origin of the Bi-concentrated and Bi-deficient bands is the kind of vacancies at Sr sites which are periodic along the *b* axis; such a model was suggested by Gay and Day [12]. In this model, it may be reasonable to assume that the added Ba ions occupy the Bi sites in Bi-deficient bands, and the possible occupation of Ba ions in BiO layers probably is responsible for the above-mentioned 4.3 nm modulation. Certainly it needs more direct experimental confirmation, and other reasons for the formation of new modulation suggested in [10, 11] cannot be ruled out. In order to clarify these problems experimentally, further observation and analyses are now undertaken.

Figure 4(*a*) shows the temperature dependence of the real component χ' and the imaginary component χ'' of the AC susceptibility for various applied DC magnetic fields H^{DC} with $f = 119$ Hz and $H_m = 0.05$ Oe for sample A. For small DC field values ($H^{DC} < 30$ G), two transitions in χ' and two corresponding loss peaks in χ'' can be seen. For the higher-T_c phase, the change in its transition temperature and width of χ' is not obvious and the height of the corresponding loss peak of χ'' increases slightly with increasing H^{DC}. However, for the lower-T_c phase, the DC magnetic field has a much greater effect on χ' and χ'', as shown in figure 4(*a*); the χ'' peak is broadened considerably and its midpoint temperature was considerably displaced. Then, for large H^{DC}-values ($30\ G \leqslant H^{DC} \leqslant 300\ G$), the transition width in χ' for the higher-T_c phase is broadened obviously, and the corresponding loss peak of χ'' is displaced by -9 K when H^{DC} increased from 30 to 300 G. However, for the lower-T_c phase, the larger DC magnetic fields appear to have a more detrimental effect; its transition in χ' and corresponding loss peak in χ'' cannot be observed within the range of measuring temperatures (65–300 K), i.e. the larger magnetic field causes such a large shift in the low-temperature peak that the midpoint temperature of the χ'' peak of the lower-T_c phase is below 65 K. We focus only on the discussion of the effect of H^{DC} on χ' and χ'' of the higher-T_c phase below.

The SEM observations suggest that the higher-T_c phase exists as a dispersed phase in the pellet surrounded by the lower-T_c phase in this sample, i.e. the higher-T_c phase grains are connected by the lower-T_c phase. Hence, there must exist weak connections between these grains of the higher-T_c phase. For this reason, the two-stage transition of the χ' curve and two corresponding χ'' peaks can be attributed to the presence of weakly coupled grains [13–16]. The low-temperature peak arises from the penetration of the magnetic field into the sections with these weak connections, and the high-temperature peak originates from the penetration of the magnetic field into grains. The diamagnetic shielding signal due to the connected lower-T_c phase is naturally much stronger than

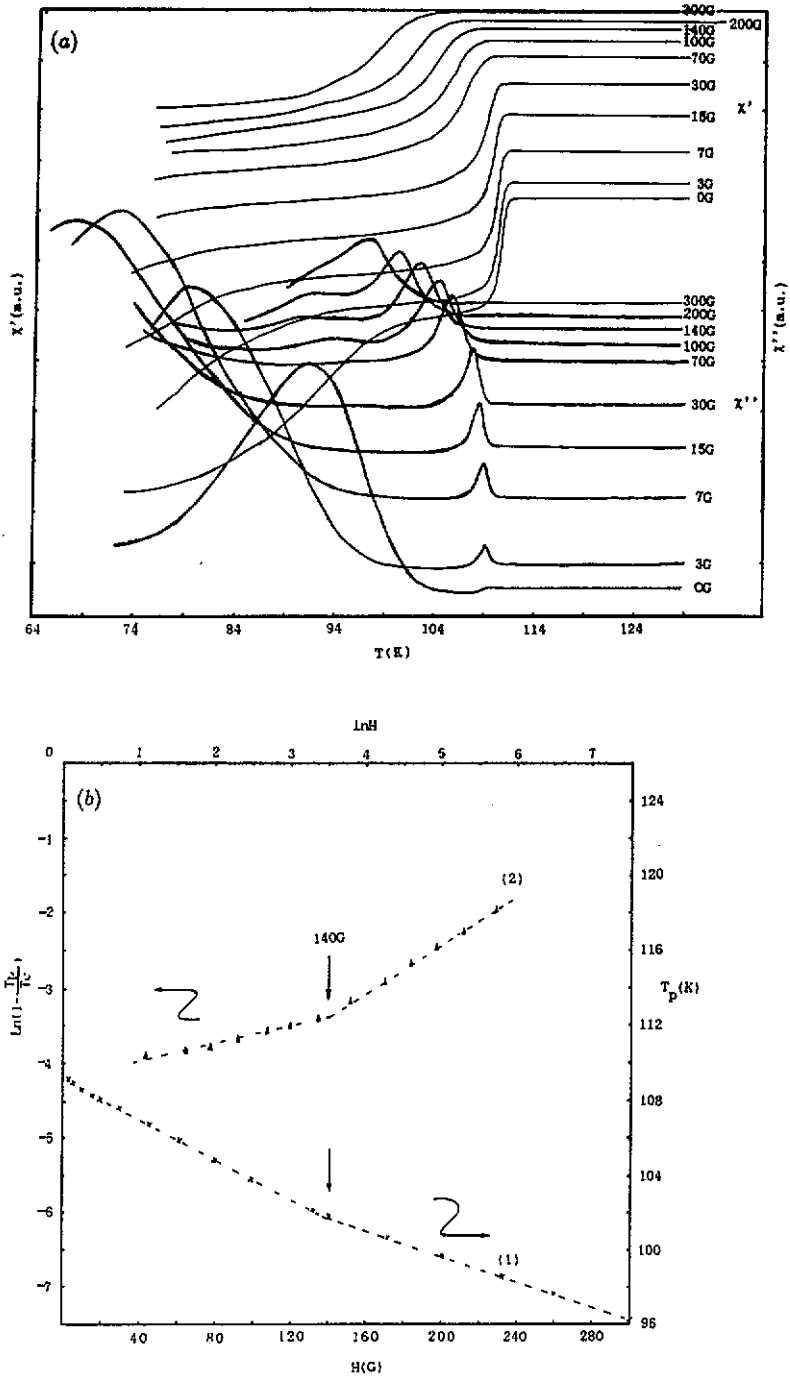

Figure 4. (*a*) The real component χ' and imaginary component χ'' of the AC susceptibility versus temperature with $H^{DC} = 0$, 3, 7, 15, 30, 70, 100, 140, 200 and 300 G for the $Bi_{1.7}Pb_{0.3}Sr_2Ca_{1.8}Ba_{0.2}Cu_3O_y$ sample. (*b*) Plots of the temperature T_p of the χ'' peak as a function of the applied magnetic field H^{DC} with H^{DC} from 0 to 300 G (curve (1)) $\ln(1 - T_p/T_c)$ versus $\ln H$ (curve (2)) (T_c is the transition temperature of χ' at $H^{DC} = 0$ G) for the $Bi_{1.7}Pb_{0.3}Sr_2Ca_{1.8}Ba_{0.2}Cu_3O_y$ sample.

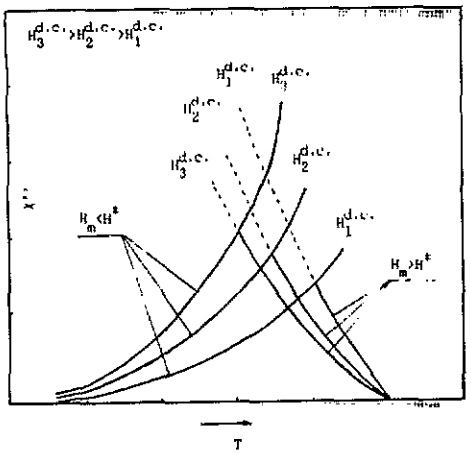

Figure 5. Typical behaviour of χ'' as a function of temperature for various applied magnetic fields H^{DC}.

that of the separated higher-T_c phase, although the amount of lower-T_c phase is much less than that of the higher-T_c phase; this phenomenon is in good agreement with our experiment results.

Since the oxide superconductors are type II superconductors, χ'' is related to the magnetic hysteresis loss caused by irreversible flux motion inside the specimen. The above-observed behaviour of χ'' for the higher-T_c phase in sample A can also be qualitatively understood in terms of Bean's critical-state model. Based on Bean's model, the relation [17] between χ'' and $J_c H_m$ can be presented as

$$4\pi\chi'' = (1/3\pi^2)H_m/J_c d \qquad H_m < H^* \tag{1}$$

$$4\pi\chi'' = 4J_c d/H_m - (16\pi/3)J_c^2 d^2/H_m^2 \qquad H_m > H^* \tag{2}$$

where d is the sample thickness and H_m is the exciting field amplitude. Since J_c is related to the applied H^{DC} and decreases with an increase in H^{DC}, the effects of H^{AC} and H^{DC} on χ'' can be considered, respectively, and H^* can be defined as the magnetic field strength at which the AC magnetic field reaches the centre of the specimen. In addition, J_c increases as the temperature decreases for a certain applied H^{DC}; as a result, the χ'' curve of temperature can be shown in figure 5 using equations (1) and (2). Then, during the transition from the normal to the superconducting state, the relation between H_m and H^* is reversed and the peak of χ'' appears schematically as shown in figure 5. The diagram deduced from Bean's model shows that the peak of χ'' shifts to lower temperatures gradually when the applied DC magnetic field value is increased, and the width and height of these loss peaks simultaneously depend on H^{DC}. The above-observed behaviours of χ'' provide experimental confirmation of the model.

The relation between $\ln(1 - T_p/T_c)$ and $\ln H$ is shown in figure 4(b) (the curve of H against T_p is also shown in figure 4(b)). From this figure, it can be found that for the higher-T_c phase the curve of $\ln(1 - T_p/T_c)$ against $\ln H$ exhibits an inflection at $H^{DC} = H_{inf} = 140$ G and cannot be fitted by $(1 - T_p/T_c) \propto H^q$ within the range of the measuring fields ($0 \leqslant H^{DC} \leqslant 300$ G); however, it can be fitted by $(1 - T_p/T_c) \propto H^{0.23}$ with $H^{DC} \leqslant 140$ G and $(1 - T_p/T_c) \propto H^{0.65}$ with $H^{DC} \geqslant 140$ G. As to the inflection in the curve of $\ln(1 - T_p/T_c)$ against $\ln H$, it can be explained as follows. According to Bean's model, H_{inf} can be really regarded as the applied magnetic field value at which the applied DC field reaches the centre of grains of the higher-T_c phase. Because the resistance

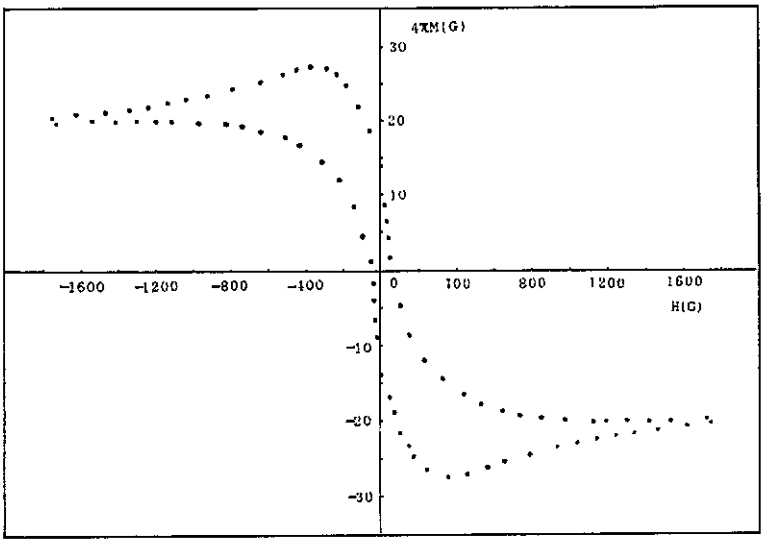

Figure 6. Magnetic moment as a function of applied DC magnetic field at $T = 77$ K for the $Bi_{1.7}Pb_{0.3}Sr_2Ca_{1.8}Ba_{0.2}Cu_3O_y$ sample.

which the fluxes encounter for $H^{DC} > H_{inf}$ is larger than that for $H^{DC} < H_{inf}$ when the fluxes penetrate into the grains of the higher-T_c phase, it is more difficult for the fluxes to penetrate into the grains of the higher-T_c phase for $H^{DC} > H_{inf}$. On the other hand, the above discussion with regard to the high-temperature peak of χ'' has indicated that the high-temperature peak of χ'' results from the penetration of the magnetic field into the grains of the higher-T_c phase. Therefore, the slope of the curve of H^{DC} against T_p is smaller for $H^{DC} > H_{inf}$ than that for $H^{DC} < H_{inf}$. This phenomenon also provides significant confirmation for Bean's model.

The DC magnetization curve of sample A is presented in figure 6. A noteworthy feature of the sample as shown by this figure is its frozen flux density B_f (at 14 G) (zero field cooled), which is much larger than that for the general Pb-doped Bi system [18]. This suggests that the content of the higher-T_c phase is larger, and the pinning centre and pinning force perhaps increase as well. On the basis of the above electron diffraction and EDS analyses,the substitutional occupation of Ba ions may result in the increase in pinning centres directly. In order to clarify the real role of the substitutional Ba ions in the crystal of higher-T_c phase experimentally, further investigations need to be made.

4. Conclusions

(i) The addition of Ba ions to a Bi–Pb–Sr–Ca–Cu–O superconductor facilitates the formation of a higher-T_c phase and a new modulation mode with a wavelength of 4.3 nm occurs simultaneously in the Ba-doped sample. Also, this kind of Ba ion substitution appears to be favourable to improvement in superconductivity; its frozen flux density and zero resistance temperature are all markedly increased.

(ii) The behaviour of the AC complex susceptibility observed in various low magnetic fields can be interpreted by employing Bean's critical-state model.

References

[1] Maeda H, Tanaka Y, Fukutomi M and Asan T 1988 *Japan. J. Appl. Phys. Lett.* **27** 209
[2] Subramanian M A, Toradi C C, Calabrese J C, Ggopalakrishnan J, Morrissey K J, Askew T R, Flippen H B, Chowdhry V and Sleight A W 1988 *Science* **239** 1015
[3] Zhangdbergen H W, Huang Y K, Menken M J V, Li J N, Kadowki K, Mennovsky A A, Vand Tendeloo G and Amelinckx S 1988 *Nature* **332** 602
[4] Toradi C C, Subramanian M A, Calabrese J C, Ggopalakrishnan J, Morrissey K J, Askew T R, Elippen R B, Chowdhry V and Sleight A W 1988 *Science* **240** 631
[5] Green S M, Jiang C, Mei Y, Luo H L and Politis C 1988 *Phys. Rev.* B **38** 5016
[6] Qinlun Xu, Tingzhu Cheng, Xiaoguang Li, Li Yang, Chenggao Fan, Haiqian Wang, Zhiqiang Mao, Dingkun Peng, Zhaojia Chen and Yuheng Zhang 1990 *Supercond. Sci. Technol.* **3** 373–6
[7] Yanagisawa E, Dietderich D, Kumakura H, Togano K, Maeda H and Takahashi K 1988 *Japan. J. Appl. Phys.* **27** 1460
[8] Mao Zhiqiang, Han Zhiyi, Wang Yu, Yang Li, Lu Jiang, Fan Chenggao, Zhou Guien, Chen Zhaojia and Zhang Yuheng 1991 *Acta. Phys. Sin.* **40** 815–20
[9] Matsui Y, Maeda H, Tanaka Y and Horiuch S 1988 *Japan. J. Appl. Phys.* **27** 372
[10] Hirotsu Yoshihiko, Tomioka Osamu, Ohkubo Tadakatsu, Yamaoto Naoki, Nakamura Yoshio, Nagakura Sigemaro, Komatsu Takayuki and Matsushita Kazumasa 1988 *Japan. J. Appl. Phys.* **27** 1869–72
[11] Matsui Yoshio, Maeda Hiroshi, Tanaka Yoshiaki and Horiuchi Shigeo 1988 *Japan. J. Appl. Phys.* **27** 372–5
[12] Gay P L and Day P 1988 *Physica* C **152** 335
[13] Couach M, Khoder A F and Monnier F 1985 *Cryogenics* **25** 695
[14] Chen D X, Goldfarb R B, Nogues J and Rao K V 1988 *J. Appl. Phys.* **63** 980
[15] Miller K-H 1989 *Physica* C **159** 717
[16] Calzona V, Cimberle M R, Ferdeghini C, Putti M and Siri A S 1989 *Physica* C **157** 425
[17] Gotoh S, Murakami M, Fujimoto H, Koshizuka N and Tanaka S 1990 *Physica* C **166** 215–20
[18] Cao Xiaoweng, Huang Sunli, Wen Haihu, Zhang Fengying, Zhang Weijie, Liu Hongbao and Zhang Yuheng 1990 *Chinese J. Low Temp. Phys.* **12** 224–9